ELSEVIER

Colloids and Surfaces A: Physicochem. Eng. Aspects xxx (2005) xxx–xxx

COLLOIDS AND SURFACES A

www.elsevier.com/locate/colsurfa

Study on the synthesis and on supermolecular structures of a water-dilutable urethane-acrylic copolymer applicable as a binder for powdered Al_2O_3

Piotr Król [a,*], Bożena Król [a], Stanisław Pikus [b], Krzysztof Skrzypiec [b]

[a] *Rzeszów University of Technology, Department of Polymer Technology, Powstańców Warszawy 6, 35-959 Rzeszów, Poland*
[b] *The Maria Curie-Skłodowska University, Faculty of Chemistry, Plac M.C. Skłodowskiej 3, 20-031 Lublin, Poland*

Received 10 October 2004; accepted 23 January 2005

Abstract

The findings were presented from the study on supermolecular structures which form spontaneously on the surface of a solidified urethane-acrylic copolymer that reveals the nature of anionomer. The isocyanate prepolymer was synthesised in the polyaddition process of 2,4- and 2,6-tolylene diisocyanate (TDI), polycaprolactone diol (PCD) and 2,2-bis(hydroxymethyl)propionic acid, and then in the reaction with 2-hydroxyethyl acrylate and 1,6-hexamethylenediamine (HMDA). At the final stage, thus, obtained urethane-acrylic macro-anionomer (UAMA) was subjected to free-radical emulsion copolymerisation with methyl acrylate and butyl acrylate to produce the aqueous emulsion of graft polyurethane-polyacrylic copolymer.

The size exclusion chromatography (SEC) method was used to evaluate distribution of molecular weights in the obtained copolymer before its cross-linking in air. The differential scanning calorimetry (DSC) and small angle X-ray scattering (SAXS) methods were employed to analyse complexity of supermolecular structures within the soft and hard domains. Also, dispersion in the continuous phase of the domains which could be observed on the surface was assessed by means of the atomic force microscopy (AFM) method.

The effects of chemical structures were discussed on diversified supermolecular structures formed spontaneously on the surface of hardened copolymer, and the resultant consequences were analysed for applicability of the produced polymer hybrids as efficient binders for powdered ceramic materials, inclusive of the most widely employed Al_2O_3.

Keywords: Polyurethane anionomers; Urethane-acrylate macro-anionomers; Chemical structure; Phase structure; SEC; DSC; SAXS; AFM; Binders for ceramic powders

1. Introduction

The scientific writings and other professional literature have for some time been reporting possible applications of water-dilutable polyurethane (PU) binders/vehicles not only for the production of environmentally friendly lacquers and/or adhesives, and for impregnation of materials with considerably high surface areas like fibrous mineral fillers, but in bonding powdered ceramic materials as well [1]. In the latter case, the task of the polymer layer is to bind the grains, e.g. Al_2O_3 grains, together when the material is subjected to pressure moulding. The polymeric binder should make possible green machining of thus pre-formed ceramic elements and give them possibly precise shapes [1]. So shaped green ceramics are then subjected to the baking process and the organic binder undergoes complete decomposition in that operation. The final and high precision complex shapes are obtained from machining of the baked product, with the use of expensive diamond tools. Polyvinyl alcohol and emulsions of some acrylic polymers have so far been used for that purpose [2]. Preliminary research findings suggest that also polyurethane polymers in the form of aqueous emulsions or dispersions could be useful. Moreover, the possi-

* Corresponding author. Tel.: +48 17 86 51579; fax: +48 17 85 43655.
E-mail address: pkrol@prz.rzeszow.pl (P. Król).

0927-7757/$ – see front matter © 2005 Published by Elsevier B.V.
doi:10.1016/j.colsurfa.2005.01.032

bility of binding powdered Al_2O_3 with aqueous PU dispersions was confirmed [3]. Our attention was also attracted by the potential use of more complex materials, i.e. hybrid poly(urethane-acrylic) polymers capable of forming water-dilutable systems. Special efforts were focused on developing dispersions on the basis of grafted poly(urethane-acrylic) ionomers which would be applicable for those outlets. Mastering the synthesis process itself for that type of systems requires precise control of the reaction stoichiometry at successive stages of the process. Still, that will not provide the final solution for the task of producing a polymeric binder which would make it possible to mould ceramic items with repeatable properties. Considerable wealth of chemical structures within oligomers that form the structure of the final urethane-acrylic copolymer affects the formation (or lack of formation) of stable aqueous systems, affects their miscibility, and affects the polymer affinity for the surface of ceramic materials as well. Moreover, the effects from chemical structures are strongly supported by the effects from supermolecular structures present in the produced systems. The effects from supermolecular structures are dependent once again on the chemical structures involved—these are determined by urethane-acrylic ionomers in our case, and additionally on the conditions adopted for moulding and cross-linking operations after the binder material has been mixed with the ceramic material at the drying stage at about 60 °C.

The microstructure of a PU block itself is generally known to be composed of different phases, i.e. it is based on domains which have been built of hard urethane-type segments and urea-derived segments, synthesised from diisocyanates and low-molecular-weight diols, amines or water, and on soft domains which have been built of flexible segments derived from polyol components [4]. Hence, additional acrylic segments, which have been built-in and which play the role of internal plasticisers, make the system even more complex. On one hand, that can be advantageous since extensive possibilities are offered to obtain the polymer structure which will be compatible with the surface of a given ceramic material. On the other hand, however, that additionally makes the manufacturing process more difficult since the need to control the chemical structure of the polymer chain is complicated by the need to control supermolecular structures when a ceramic item is being moulded. Still, supermolecular structures within hybrid polymers themselves must be learned initially and that problem makes the basic focus of this paper. The question has been investigated by means of modern methods of instrumental analysis: differential scanning calorimetry (DSC), wide angle X-ray (WAX) scattering, small angle X-ray scattering (SAXS) and atomic force microscopy (AFM), which have already been employed earlier for the analysis of supermolecular structures in urethane and acrylic polymers [4–6].

Within those techniques, only the AFM method, which records interactions between a measuring tip and the sample, offers the possibility of accurate visualisation of structures, i.e. the possibility of imaging the sample with visible hard and soft domains, with various shapes, various size and arrangement over the sample surface. Depending on the detection technique, those images show the mechanical (roughness, friction factor) or chemical nature of the surface (wettability, polarity) [7].

Irrespective of application-related questions as mentioned above, learning the surface structures of urethane-acrylic ionomers enhances our knowledge on physical interactions between chain segments. These interactions can also be essential for other applications of that type of materials. When water-repellent alkyl structures are incorporated into the PU macromolecules, it becomes possible for example to precipitate polyurethane particles from organic solutions. The particles will not agglutinate and after the drying operation they can be employed as environmentally attractive powder coatings [8]. Moreover, poly(urethane-acrylic) dispersions which have the characteristic of interpenetrating polymer networks (IPN systems) find their outlets as tight protective coatings [9,10].

2. Experimental

2.1. Raw materials

2,4- and 2,6-Tolylene diisocyanate (TDI), technical product from Aldrich.

It was a mixture of 2,4-TDI and 2,6-TDI isomers at the ratio of 80 and 20%, respectively. The raw material was used as purchased.

Polycaprolactone diol (PCD) (reagent from Aldrich)

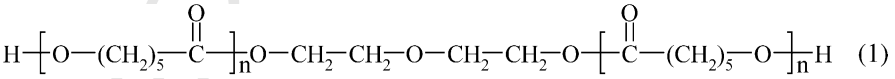

(1)

- M_n = 530 g/mol;
- Density = 1.073 g/cm^3;
- Softening temperature = 35 °C.

The product was dewatered by holding it at temperature of 80 °C under the pressure of 20 mmHg over 120 min.

Triethylamine (purity 99.5%) (reagent from Aldrich). The reagent was used as purchased.

2,2-Bis(hydroxymethyl)propionic acid (98%) (DMPA) (reagent from Aldrich)

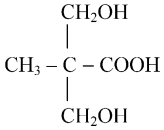

Melting point 190 °C. Hygroscopic product. That reagent was dried directly before its use in a cabinet drier, at 120 °C.

1,6-Hexamethylenediamine (HMDA) (98%) (reagent from Aldrich). The reagent was used as purchased.

2-Hydroxyethyl acrylate (HEA) (96%) (reagent from Aldrich)

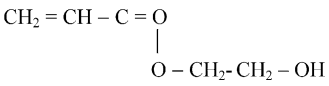

The reagent was used as purchased.

- Methyl acrylate (99%) (MA) (reagent from Aldrich);
- Butyl acrylate(99%) (BA) (reagent from Aldrich).

The purchased MA and BA monomers contained about 10–55 ppm of monomethyl ethyl hydroquinone. That level is sufficient to prevent spontaneous polymerisation, yet it is too low to prevent polymerisation induced by any additional initiator. Hence, the acrylic monomers were used directly as purchased.

N,*N*-dimethylformamide (DMF) (99.8%) (reagent from POCh S.A., Gliwice, Poland). Boiling point 153 °C. The material was dewatered by azeotropic distillation with benzene, and then stored over molecular sieves type 4A from POCh S.A., Gliwice, Poland.

Tetrahydrofuran (THF) (99%) (reagent from POCh S.A., Gliwice, Poland). Boiling point 67 °C. The material was dewatered by distillation in the presence of sodium metal, and then stored over molecular sieves type 4A.

Hydrogen peroxide (30% solution in water) (reagent from POCh S.A., Gliwice, Poland). The reagent was used as purchased.

Formic acid (96%) (reagent from POCh S.A., Gliwice, Poland). The reagent was used as purchased.

3. Manufacturing method for poly(urethane-acrylic) macro-anionomer

All the synthesis processes were carried out in a glass stand, i.e. in a three-necked flask provided with a magnetic stirrer, dropping funnel, thermometer, reflux condenser as well as nitrogen supply point. The poly(urethane-acrylic) macro-anionomer product was synthesised in a four-staged step-growth polymerisation process, followed by free-radical copolymerisation in aqueous emulsion.

3.1. Stage I—synthesis of isocyanate prepolymer (AB_2)

Urethane-isocyanate prepolymer was obtained by adding molten PCD drop by drop to the flask where TDI had been placed previously. The temperature of PCD was maintained at 60 °C by means of an IR radiator. That stage can be illustrated as follows:

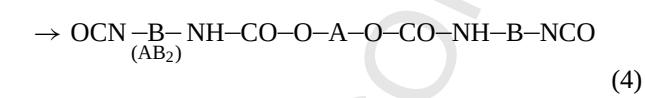

(4)

where A is the segment derived from PCD structure (1); B, the segment derived from TDI structure.

Dropwise addition of PCD at 60 °C took 20 min. The resulting mixture was then maintained at 75 °C over 60 min, under a reflux condenser and dry nitrogen. After the reaction had been completed, the mixture was cooled down to 50 °C. The content of –NCO groups was then determined as 10.09% (the stoichiometrically calculated value is 9.56%).

3.2. Stage II—synthesis of urethane-isocyanate anionomer (UIA)

Urethane-isocyanate anionomer (UIA) was synthesised with the use of DMPA as a chain extender for the AB_2 prepolymer:

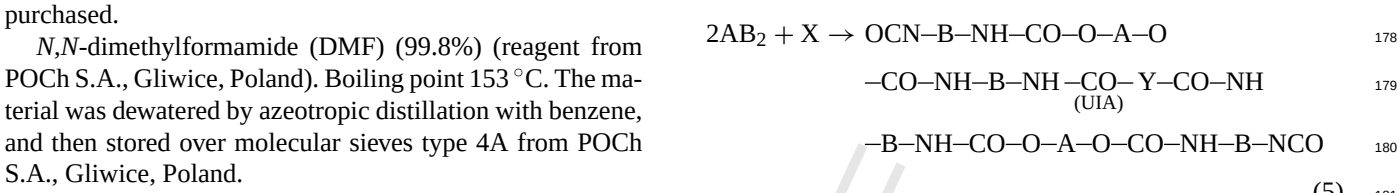

(5)

where X is the DMPA (2); and Y, the segment derived from built-in DMPA.

DMPA was added to the reactor in the form solution in DMF (1:7). The reaction was continued at 50 °C over 60 min. The obtained prepolymer contained 2.81% –NCO groups as titrated with the use of dibutylamine (calculated value is 2.70%) [11].

3.3. Stage III—synthesis of urethane-acrylic macro-anionomer (UAMA)

UIA was reacted with HEA to yield urethane-acrylic macro-anionomer (UAMA) with acrylic end groups, which contained 0.2% unconverted isocyanate groups [11].

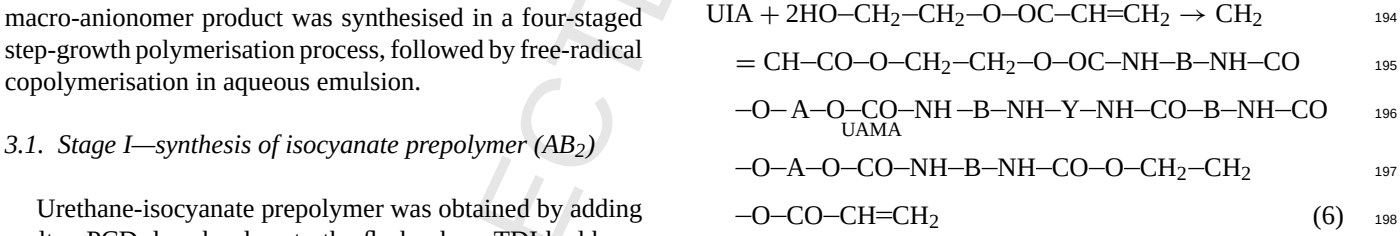

(6)

The reaction took 90 min at 50 °C.

3.4. Stage IV—synthesis of ammonium salt of urethane-acrylic macro-anionomer

At this stage, the reaction of UAMA macro-anionomer carboxyl group (structural fragment Y) and TEA yielded the triethylammonium cation. That reaction can be represented by the following equation:

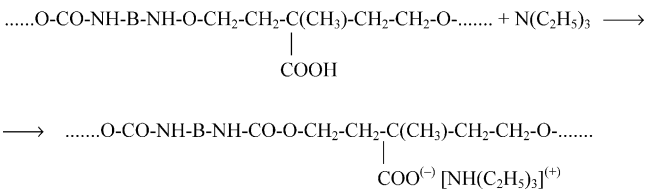

The macro-anionomer produced in that way was capable of forming aqueous dispersions. The obtained UAMA with the number of –COOH groups known from stoichiometric calculations was reacted with the equimolar amount of TEA. The amine was added at 30 °C until the level of pH 7.5 was reached.

The UIA isocyanate anionomers which were left unconverted from stage III were then extended by means of HMDA. The major amount of HMDA (90%) was added in the form of solution in THF, at room temperature. The reaction was then continued at 30 °C over 90 min, and the content of –NCO groups was analysed once again (0.08%) [11]. Residual –NCO groups, which were not completely converted, demanded the use of aqueous dispersion and a small amount of HMDA:

$$\cdots Z\text{–}CO\text{–}NH\text{–}B\text{–}NH\text{–}CO\text{–}O\text{–}A\text{–}O\text{–}CO\text{–}NH\text{–}B\text{–}NCO + nH_2N\text{–}(CH_2)_6\text{–}NH_2 \rightarrow Z\text{–}NH\text{–}CO\text{–}NH\text{–}B\text{–}NH\text{–}CO\text{–}O\text{–}A\text{–}O\text{–}CO\text{–}NH\text{–}B\text{–}NH\text{–}CO\text{–}NH\text{–}(CH_2)_6\text{–}NH_2 \quad (8)$$

where Z is the segment derived from UAMA macro-anionomer structure.

The mixture was then subjected to mechanical dispergation during another 30 min, at room temperature: intense agitation was applied with the dropwise addition of re-distilled water. THF was subsequently recovered from the obtained emulsion by means of distillation. The dry matter content in the produced aqueous-THF–DMF emulsion was determined by gravimetric analysis after evaporation of solvents in a drier, at 120 °C over 120 min. That was found to amount to 26.5 wt%.

3.5. Stage V—copolymerisation of urethane-acrylic macro-anionomer with acrylates

The free-radical copolymerisation process, in which aqueous emulsion of UAMA and mixed MA + BA monomers were involved, yielded the poly(urethane-acrylic) macro-anionomer, i.e. the final product (FP) of our synthesis. For that purpose, an aqueous emulsion of poly(vinyl alcohol) (10%), acidified with HCOOH to pH 2–3 and containing the redox initiator system: $FeSO_4 \cdot 7H_2O$ (0.1 wt%) and H_2O_2 (2 wt%), was prepared. Then MA and BA monomers as well as the UAMA emulsion from stage IV were charged to said initial emulsion. The volumes of those components were adjusted to obtain the molar ratio of their vinyl groups (–CH=CH_2) of 5:1:1, respectively. The polymerisation process was performed at 80 °C over 3 h, at a constant speed of the agitator, and under nitrogen to prevent any oxidation of vinyl groups with atmospheric oxygen. The polymer content in the produced emulsion was brought to 30 wt% by adjusting the volume of re-distilled water added to the system. The dry matter content in the FP copolymer, as determined by gravimetric analysis, amounted to 30.2 wt%.

4. Testing equipment and analytical methods

4.1. Determination of –NCO group content

That determination involved a well-known method, and dibutylamine was used in the tests. Excess of unreacted amine was titrated with the HCl solution and bromophenol blue was used as an indicator [11].

4.2. Size exclusion chromatography (SEC)

The size exclusion chromatography (SEC) analyses of UIA and UAMA polymers were performed using a JASCO HPLC pump type 880-PU, TOSOHAAS 3 columns of TSK gel Hhr (2000, 3000, and 4000 Å) filled with a new polystyrene divinylbenzene gel, Varian (series RI-3) refractive index detector, and with DMF as a mobile phase (flow rate: 0.7 cm^3/min), at room temperature. The system was calibrated by means of narrow molecular weight polystyrene standards.

4.3. Differential scanning calorimetry (DSC)

A Mettler Toledo type 822^e differential calorimeter (DSC) with Star^e System software was employed to analyse thermal properties of cured PUs. The instrument was calibrated with the use of Zn and In standards.

The samples were placed in aluminium crucibles. These were weighed to the nearest $0.0001 \times g$ and placed in the measuring chamber. Initially, the samples were heated up to 60 °C to eliminate stresses which possibly could be left after the moulding process, and then they were cooled down to −80 °C. After another 10 min, their progressive heating was initiated at the rate of 10 deg/min. The measurements were taken within the temperature range of from −80 to 250 °C, in the environment of nitrogen which was passed at the rate of 30 cm^3/min.

Temperatures for phase transitions (T_m, T_g) and the values for enthalpy of fusion ΔH_m were found by means of a generally known method.

4.4. WAXS and SAXS analysis

The wide angle X-ray scattering (WAXS) investigations involved the use of Seifert URD-6 diffraction instrument. The radiation of Cu Kα and the nickel filter were employed. The operating conditions for the instrument were as follows:

accelerating voltage −40 kV, anode current −30 mA. X-ray diffraction patterns were taken within the range of 2Q from 1° to 60°, at the increments of 0.1°, and at counting intervals of 10 s.

SAXS measurements were performed on a slit-collimated Kratky camera using a Cu anode tube as the radiation source. A proportional counter with a nickel filter and a pulse-height analyser were used. As a result of the measurements, the curve – intensity of scattering $J(q)$ versus module of scattering vector q – was obtained:

$$q = \frac{4\pi \sin\theta}{\lambda} \quad (9)$$

where 2θ is the scattering angle; λ, the X-ray wavelength (1.542 Å).

4.5. Analysis of superficial structures by means of AFM method

The atomic force microscope (Nanoscope III, Digital Instrument, USA) was employed to study superficial structures of the coating obtained from FP. The scans were taken at ambient temperature, in air, and in contact mode (CM) conditions, i.e. at direct contact between the sample surface and the tip. The pyramidal Si_3N_4 tip employed in the CM system has a spring constant of 0.06 N/m (Nanoprobe™). Each scan was presented in the following data formats:

- topographic image (height, *h*), two-dimensional or three-dimensional (3D);
- phase image (phase, p), which represents the phase lag for probe vibrations at the boundary between two media due to friction of the probe/needle tip on the sample surface (friction, *f*) or axial deflection z of the probe/needle tip after it hits any surface irregularity (deflection, *d*).

In order to provide additional information on the most interesting superficial phenomena and sudden changes in surface topography of the sample as observed in the image presented in Fig. 7, the sectional analysis was performed along the A–A′ line.

The cover layer to be studied was obtained by careful evaporation of water from the FP dispersion at 120 °C during 2 h. Evaporation of water was confirmed by comparing the sample weight before and after evaporation (the evaporation operation took 1 h). After one more hour of drying, the sample weighing operation was repeated.

5. Discussion of results

The adopted method of multi-staged synthesis has been intended to yield the block structure of polyurethane chains since that structure is favourable for separation of soft and rigid segments [12]. It is possible to obtain a regular structure but the reaction stoichiometry needs to be controlled at every successive stage of the polyaddition process. It is known from the assumed stoichiometry that the produced chains are composed of a known share of soft segments (about 43.4 wt% on FP), derived from PCD, which have been connected by means of urethane groups to aromatic (hard) structures derived from TDI. The short-chained acid, DMPA, provides –COOH groups which are evaluated to make 1.8 wt%. However, the macromolecules can become even more rigid due to the presence of those groups since they are also involved in the formation of a system of hydrogen bonds. Additionally, ionic groups – when neutralised with TEA-derived and more mobile ammonium counter-ions – are responsible for improved hydrophilic properties, improved affinity of ionomer for water, and for improved electric conduction of aqueous dispersion. The HEA-derived acrylic segments (9.03 wt%) can be expected to exhibit a more softening effect, just alike ethyl groups in TEA, and they will act jointly in this respect with PCD soft segments. As results from the calculations based on the mass balance and stoichiometry for individual reactions, the total share of the softening structures reaches to about 57 wt% in FP. On the other hand, the small amount of HMDA which has been additionally built-in into the prepolymer chain must certainly be responsible for introducing urea-type polar groups and hence, for stiffening of the system. However, the share of such structures is reasonably low (about 0.6 wt%) since stage III was controlled to leave less then 2 mol% of unconverted –NCO groups which would then be capable of reacting with HMDA in stage IV.

As can be seen from the above data, the share of hard segments in the obtained FP copolymer reaches to about 43%. Those structures are composed of TDI-derived urethane segments, small amounts of TDI and HMDA-derived urea-type segments, and also AM and HEA-derived polar acrylic groups.

The molar ratio of co-monomers, i.e. UAMA, AM and AB, of (5:1:1) adopted for the polymerisation mixture offered equal chances of incorporating any vinyl monomer into the FP chain during the free-radical copolymerisation process. The HEA, AM and AB-derived acrylic segments made up about 13.5 wt% of FP in total. The use of AB monomer molecules was planned to counterweight the effects from polar acrylic structures responsible for stiffening of the structure with non-polar and softening n-butyl groups.

Thus, obtained linear poly(urethane-acrylic) macroanionomer (FP) was characterised by very complex structure of its chain that had been made up of hard and soft segments with diversified polarity. That polymer was applied in the form of aqueous dispersion on a solid substrate (glass) and it was dried in air at 60 °C. In effect, it was subject to cross-linking in accordance with a typical oxygen-involving radical mechanism, and thus, it was converted into a material which was no longer soluble, neither in water nor in DMF (polar solvent). Hence, it was impossible to make use of the SEC method to determine its molecular weight. So, its structure as discussed above is hypothetical only and the specified weight percentages for individual segment types have been

calculated on the basis of the material balance for the whole process.

However, SEC chromatograms were taken for intermediate products obtained from stage II (UIA) and stage III (UAMA) (Fig. 1). They provide a general outlook only as regards polydispersity of the studied polymers. We failed to arrive at precise quantitative conclusions due to a too low – as we finally found out – top limit adopted for the calibration curve. It can be seen from the collected data that the UIA anionomer resulting from stage II offers a relatively narrow molecular weight distribution (MWD). On the other hand, MWD for UAMA is much wider what seems to result most probably from the HEA addition stage. Hence, it is clear that the linear FP is characterised by even higher polydispersity and structural diversity directly after its separation from aqueous emulsion, before its cross-linking in the presence of oxygen. That complex chemical composition of FP must be decisive for its ultimate phase structure and supermolecular structure which are formed during its spontaneous solidification after FP has been applied to a substrate surface.

The supplementary information on the presence of rigid and flexible segments in the FP copolymer became available due to the use of the DSC method. As can be seen in thermogram presented in Fig. 2, FP is composed also of the soft phase with the glass transition point of $T_{g1} = -62.4\,^{\circ}C$. That low range of glass transition is specific for PU elastomers and it results from the presence of soft polyol-type segments, PCD segments in this case [12]. Another glass transition point observed in the positive range ($T_{g2} = 2.1\,^{\circ}C$) probably makes the evidence for low miscibility of said soft segments and hard urethane-type segments which usually form the hard phase with $T_{g3} > 20\,^{\circ}C$ in PU elastomers [13]. That phase can not be declared present in FP on the basis of DSC thermogram. That can be explained just by the effect from acrylates as discussed above, and in particular from AB, which plasticise the hard phase in PU. What is especially noteworthy is a wide endo peak within 60–110 °C which makes the indication of some orderly arrangement of the hard phase in PU. Thus, the DSC findings provide another premise for a diversified nature of supermolecular structures in the synthesised polymer. We hoped for further clarification of that problem by measuring X-ray diffraction for the samples of coatings obtained from the FP copolymer.

The SAXS pattern shows a clear maximum for the scattering vector $q = 0.035\,\text{Å}^{-1}$ (Fig. 3) what makes it possible to calculate the linear parameter for orderly arranged aggregates $d = 179\,\text{Å}$ which create the internal structure of the hard domain considered. This finding confirms that the FP copolymer features polydispersity of supermolecular structures within the area of aggregated hard segments. That issue is even more interesting since a similar nature for the SAXS curve was obtained for the PU elastomer in which hard segments had been created by model urethanes derived from 1,4-butanediol and piperazine [soft segments in that PU had been produced of poly(tetramethylene oxide)]. The recorded value for $d = 106\,\text{Å}$ was assumed to correspond to interdomain spacing between the hard segment structures within the hard domain [9]. In our case, however, the interdomain structures were much more complex what was confirmed by the appearance of the second and more flat maximum at $q = 0.054\,\text{Å}^{-1}$

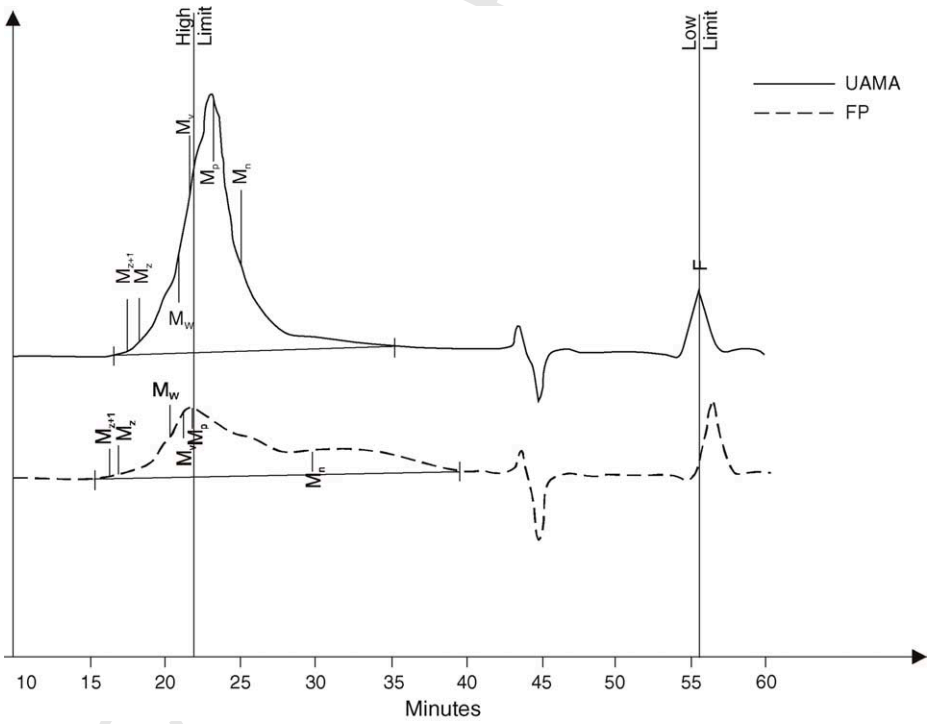

Fig. 1. SEC chromatograms of UIA and UAMA ionomers.

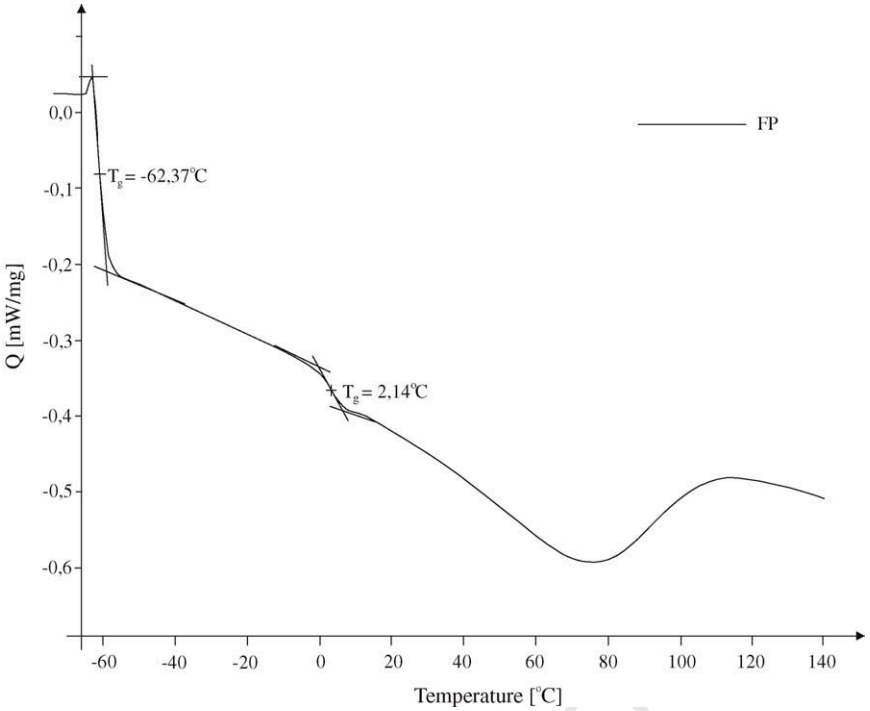

Fig. 2. DSC thermogram of FP copolymer.

($d = 116$ Å) (Fig. 3). That could be accounted for by some additional interdomain spacing which could result from still another hard segments. The analysis of SAXS patterns with similar profiles for ionomers based on copolymers of styrene and acrylic acid suggests that the first interference maximum ($q = 0.1$ Å^{-1}) corresponds to bigger ionic aggregates wherein the clusters have the diameter within 50–100 Å. However, the second maximum ($q = 0.3$ Å^{-1}) appears only for more than 11.7 mol% acrylates with built-in Cs^+ counter-ions, and it results from the presence of smaller particles (the so-called multiplets) with the diameter below 40 Å [5]. The interdomain spacing specific for our FP copolymer, with a somewhat smaller size only, can thus result from the presence of hard acrylic segments. Those segments are more numerous than the urea-type ones and their structures are more diversified at the same time since the structures can be formed by copolymers derived from the combination of HEA and AM. And the copolymers can interact through dispersion forces with carboxyl ions with built-in TEA counter-ions.

The WAXS pattern (Fig. 4) confirms the above conclusions. Two peaks have been outlined in it. The first one is very wide, it has been recorded for a lower value of angle 2Θ, and

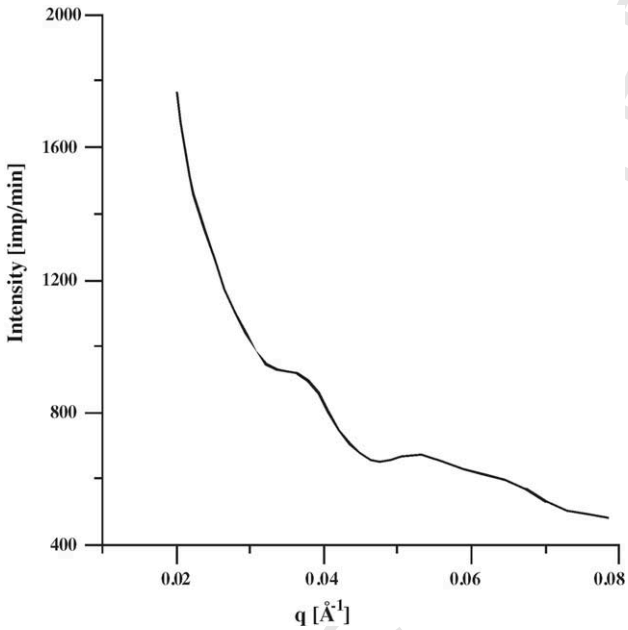

Fig. 3. SAXS spectrum of FP copolymer.

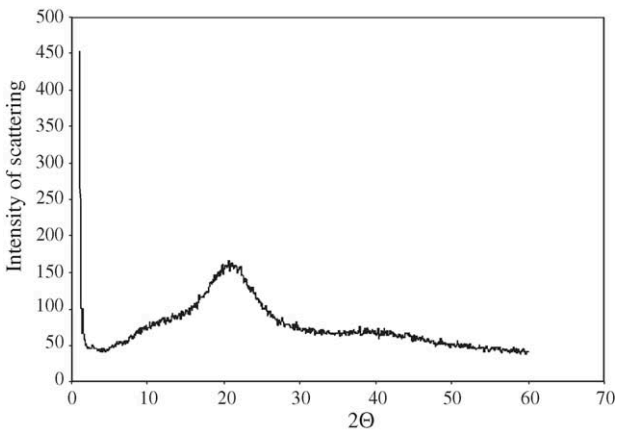

Fig. 4. WAXS spectrum of FP copolymer.

it makes the evidence for the presence of a poorly ordered phase with more loose packing. The other one is clearly not so wide, it has been recorded at a higher value of 2Θ, and it proves the presence of an orderly arranged phase with close packing. One could expect that such a complex intradomain structure can appear within hard domains with various size, shape and dispersion within the matrix of FP copolymer. It should expectedly be best observed in a thin film of polymer coating. Hence, we found it advisable to go to visualisation of superficial microstructures of a cross-linked film with the use of the AFM technique.

Figs. 5a and 6a show three-dimensional AFM images for topography of FP surface samples of 30 μm × 30 μm and 10 μm × 10 μm, respectively, while the corresponding two-dimensional images have been shown in Figs. 5b and 6b. Those figures demonstrate a strongly diversified topography within even respectively small surface fragments of the analysed samples. The light-coloured places represent hard domains which are grouped into compact areas having the size of from 0.5 to 2.0 μm. Sometimes, however, they are dispersed all over the matrix which is formed by soft domains. Miscibility of hard and soft segments forming both types of domains is apparently limited and that limitation is more clearly seen at the interphase. The differences in height (h)

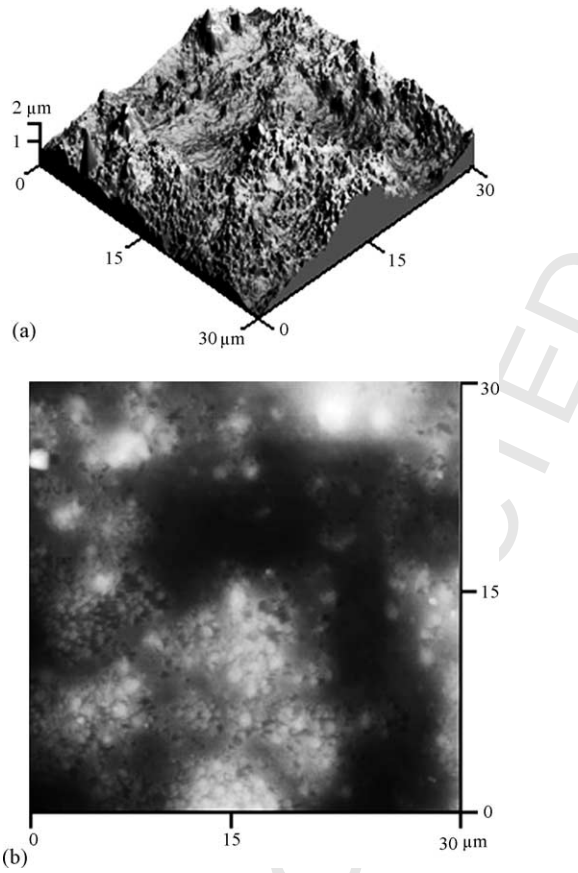

Fig. 5. (a) Three-dimensional AFM image of a 30 μm × 30 μm surface area of FP sample (b). Two-dimensional AFM image of a 30 μm × 30 μm surface area of FP sample.

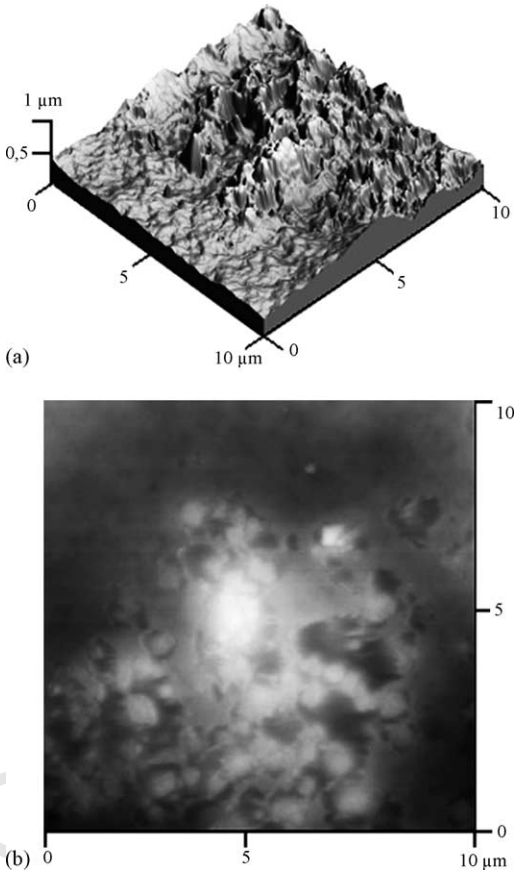

Fig. 6. (a) Three-dimensional AFM image of a 10 μm × 10 μm surface area of FP sample (b). Two-dimensional AFM image of a 10 μm × 10 μm surface area of FP sample.

(light-coloured and dark places) reach as high as 2500 nm. The most light-coloured details of topography in the obtained AFM image represent the particles with the diameter of about 100 nm (Fig. 6a). These can be attributed to linear dimensions of individual hard domains formed (light-coloured agglomerations against the dark background) or soft domains formed (dark-coloured against the light or grey background).

Fig. 7 provides the 10 μm × 10 μm AFM image scan of the analysed surface. Those image result from the changes in physical properties, e.g. mechanical features or surface friction, experienced when a sample is analysed with the use of the AFM method. Single inclusions or whole agglomerates of hard domains are visible on the background of dark-coloured or grey polymer matrix formed by soft segments. The analysis of the phase image (Fig. 7) suggests that the domains which produce sharply outlined heights in the topographic picture (Fig. 6a and b) are not composed – as one might expect from h-type images (3D or 2D) – solely of hard segments. Hard segments are also to some extent dispersed within the matrix of FP copolymer. That AFM image is clearly different from a typical image for a segmented PU elastomer as observed with that technique, in which domains of hard segments and domains of soft segments can be clearly observed [4,8]. We face a better dispersed structure in FP copolymer which probably

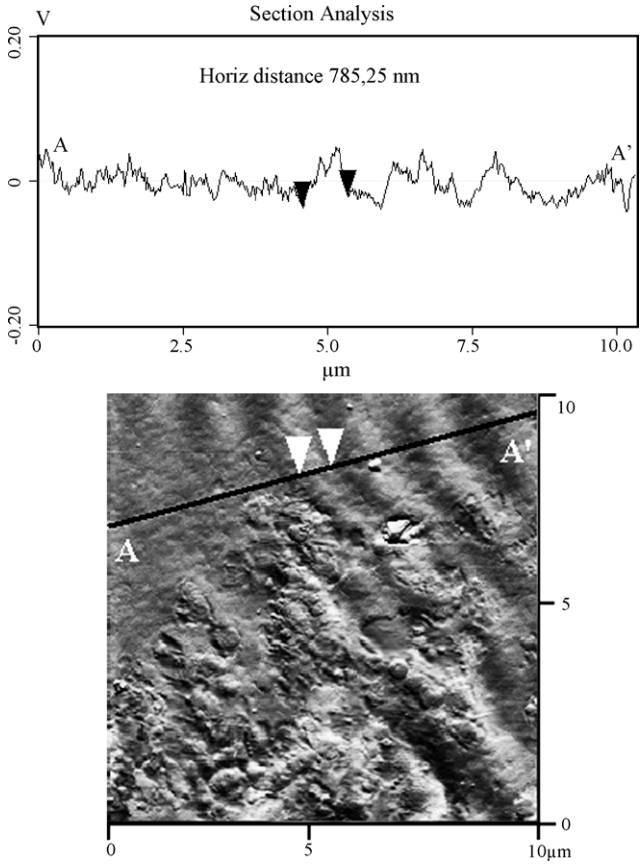

Fig. 7. AFM phase image (friction) of a 10 μm × 10 μm surface area of FP sample. Section. analysis of structures observed in AFM image of FP copolymer.

results from the presence of acrylates, HEA, AB and MA, and from the presence of ionic groups. The former components exert the softening action while the later bring their contribution both into stiffening the structures through ionic bonds and hydrogen bonds, and into softening the structures at the same time through water-repellent alkyl groups of built-in acrylates and additionally TEA counter-ions. Inclusions or even agglomerates of hard segments can be seen in some limited areas. In just those areas probably there existed the possibility of better orientation what was manifested in the form of diffraction maximum in the SAXS curve (Fig. 3).

The AFM image (Fig. 7) generally shows that the structure of FP copolymer has been composed of a relatively homogeneous matrix, into which shapeless hard domains have been included in the form w single "islands". The mass fraction of that reasonably well developed hard phase can be evaluated at 25–30%, hence, the balance 8–13% of hard segments must be dispersed in the soft phase.

There are strongly non-uniform and tumour-like structures in the AFM image (Fig. 7) which have been built-in into the matrix. In order to be able to investigate that image more closely, we analysed a section along the line A–A′. The width of that excrescence was indicated by markers. The AFM analyser recorded considerable fluctuations in superficial properties along that line what makes the evidence for actual diversification of the surface. That can result from immiscible hard domains and soft domains located close to each other and overlapping with each other.

6. Summary

Inserting HEA into the PU ionomer with a relatively compact structure as obtained from the controlled polyaddition process of TDI, PCD and DMPA, is responsible for substantially increased polydispersity and structural inhomogeneity of the formed UAMA product. That inhomogeneity, in turn, is shown by the complex supermolecular structure of FP poly(urethane-acrylic) macro-anionomer obtained from the free-radical copolymerisation process of UAMA macroionomer with AM and AB acrylates.

Within the supermolecular microstructures which can be observed with the use of DSC and SAXS methods, there is the soft phase which is derived from PCD soft segments with T_g = –60 °C, and the hard phase as well which is formed not only by hard urethane segments – what is the case for segmented PU elastomers – but also by urethane segments mixed together with acrylic segments, which can both stiffen the structure due to the presence of more polar acrylic groups and have the softening effect owing to their alkyl groups. The hard segments form orderly arranged structures, grouped into hard domains observable in AFM images, but some of them are also pretty well dispersed within soft domains which form the principal matrix of the FP copolymer. The superficial structure of the film of so obtained material is, hence, inhomogeneous: it is formed both by very small domains, with the size of between 10 nm and 20 nm, and by 100–200 nm agglomerates as well which are arranged within the domains of the more compact phase composed of soft domains.

The observed structure was formed in the spontaneous and unforced way, by slow evaporation of water from the polymer dispersion, and so it offers superior durability which probably results from strong electrostatic and polarisation interactions between ions and functional groups of hard segments dispersed in soft domains and clustered in hard domains.

Hence, the supermolecular structures in the FP copolymer are dependent on its chemical composition and on the film formation conditions, i.e. conditions for water evaporation from the dispersions and for film cross-linking. Analogous structures will most probably be formed when the FP cationomer is used to fix together the grains of ceramic materials, e.g. Al_2O_3, in the ceramic product pressure moulding process. The use of ionomers, and specifically urethane-acrylic anionomers, in the production of such binders for green ceramics is expected to be advantageous since polar ionic bonds can be formed between the polymer and the surface of Al_2O_3 grains which is alkaline.

Further studies will be oriented on finding the correlation between the supermolecular structures formed in the interphase between the layer of FP copolymer and ceramic

grains, and mechanical properties of green ceramics formed (moulded) with the use of a binder produced of above described polyurethane anionomers.

Acknowledgement

This study was performed within the research project No. 7 T09B 12722 which was financially supported by the Committee for Scientific Research in Warsaw.

References

[1] D.B.R. Kumar, R.M. Reddy, V.N. Mulay, N. Krishnamurti, Eur. Polym. J. 36 (2000) 1503.
[2] X.L. Wu Kewin, J. Mc Anany, Am. Ceram. Bull. 74 (1995) 61.
[3] M. Potoczek, M. Heneczkowski, M. Oleksy, Ceram. Int. 29 (2003) 259.
[4] A. Aneja, G.L. Wilkes, Polymer 44 (2003) 7221.
[5] K. Suchocka-Gałaś, C. Ślusarczyk, A. Wlochowicz, Eur. Polym. J. 36 (2000) 2167.
[6] I. Revenko, Y. Tang, Santerre.: Surf. Sci. 491 (2001) 346.
[7] H. Janik, B. Pałys, Z.S. Petrovic, Macromol. Rapid Commun. 24 (2003) 265.
[8] B. Radhakrishnan, P. Chambon, E. Cloutet, H. Cramail, Colloid Polym. Sci. 281 (2003) 516.
[9] B.K. Kim, K. Tharanikkarasu, J.S. Lee, Colloid Polym. Sci. 9277 (1999) 285.
[10] M. Hirose, J. Zhou, K. Nagai, Prog. Org. Coat. 38 (2000) 27.
[11] H.E. Stagg, Analyst 71 (1966) 557.
[12] E.G. Bajsic, V. Rek, A. Sendijarevic, V. Sendijarevic, K.C. Frisch, J. Elastomers Plast. 32 (2000) 162.
[13] I.H. Kim, J.S. Shin, I.W. Cheong, J.I. Kim, J.H. Kim, Colloids Surf. A: Phys. Eng. Aspects 207 (2002) 169.